International Journal of Thermophysics, Vol. 16, No. 1, 1995

A Fundamental Equation of State for 1,1-Difluoroethane (HFC-152a)[1]

R. Tillner-Roth[2]

A fundamental equation of state for HFC-152a (1,1-difluoroethane) is presented covering temperatures between the triple-point temperature (154.56 K) and 435 K for pressures up to 30 MPa. The equation is based on reliable (p, ϱ, T) data in the range mentioned above. These are generally represented within $\pm 0.1\%$ of density. Furthermore, experimental values of the vapor pressure, the saturated liquid density, and some isobaric heat capacities in the liquid were included during the correlation process. The new equation of state is compared with experimental data and also with the equation of state developed by Tamatsu et al. Differences between the two equations of state generally result from using different experimental input data. It is shown that the new equation of state allows an accurate calculation of various thermodynamic properties for most technical applications.

KEY WORDS: equation of state; Helmholtz free energy; HFC-152a; refrigerants.

1. INTRODUCTION

1,1-Difluoroethane (HFC-152a) is an alternative refrigerant which is suitable as a substitute for CFC-12. Due to its flammability, this fluid has not seen widespread use in the refrigeration and air-conditioning industry. However, its zero ODP (ozone depletion potential) and very low GWP (greenhouse warming potential) make it an interesting ozone-friendly refrigerant for applications where its hazards can be kept under control. Furthermore, it is used as a component of mixtures to enhance cycle performance and to lower the GWP of the total charge of a refrigeration cycle.

[1] Paper presented at the Twelfth Symposium on Thermophysical Properties, June 19–24, 1994, Boulder, Colorado, U.S.A.

[2] Institute of Thermodynamics, University of Hannover, Callinstrasse 36, 30167 Hannover, Germany.

0195-928X/95/0100-0091$07.50/0

As with many of the ozone-friendly CFC substitutes, the thermodynamic properties of HFC-152a have been extensively investigated in recent years. In this paper, an equation of state is presented which is based on the most reliable of experimental data and which accurately represents the thermodynamic properties of HFC-152a for temperatures between 154.56 and 435 K at pressures up to 30 MPa.

2. EXPERIMENTAL DATA

A large number of measurements of the thermodynamic properties are available in an extended range of pressure and temperature. A detailed survey of available sources is given by Tillner-Roth [1]. About 1700 (p–ϱ–T) values were reported for temperatures between 160 and 453 K and pressures up to 60 MPa, covering the liquid and the vapor regions. Caloric measurements are not available to that extent. There are only three sets of isobaric heat capacities measured in the liquid region for temperatures between 225 and 423 K at pressures between 2 and 20 MPa. Speed of sound values were measured in the vapor phase only below 0.5 MPa [2], with the aim to determine the ideal-gas heat capacity. No caloric measurements are known in the liquid below 220 K and there is also a gap in the vapor between 0.5 and 2 MPa, especially for supercritical temperatures.

Extensive investigations have also been carried out on saturation properties for a total of 380 vapor pressures, 116 values for the saturated liquid density, and 38 saturated vapor densities. These measurements extend from the triple-point temperature (154.56 K) to the critical temperature (386.41 K) except for the saturated vapor density, which has not been measured below 335 K.

The fundamental equation of state is based on the following experimental data:

- 702(p–ϱ–T) values measured by Tillner-Roth and Baehr, [3, 4] in the liquid between 243 and 413 K and in the vapor between 293 and 433 K at pressures up to 16 MPa,
- 206(p–ϱ–T) values in the liquid reported by Blanke and Weiss [5] between 160 and 434 K at pressures up to 30 MPa,
- 109(p–ϱ–T) values measured by Dressner and Bier [6] at 333 and 373 K below vapor pressure and at 423 K at pressures up to 58 MPa,
- 306 c_p-values at high densities measured by Porichanskii et al. [7] between 225 and 423 K at pressures between 2 and 20 MPa,

- 91 vapor pressures measured by Baehr and Tillner-Roth [8] and by Blanke and Weiss [5] covering the whole two-phase boundary, and
- 19 saturated liquid densities measured by Blanke and Weiss [5] between 160 and 308 K.

Further details on the selection of these measurements are given by Tillner-Roth [1].

3. THE FUNDAMENTAL EQUATION OF STATE

The equation of state for HFC-152a is a fundamental equation of state for the dimensionless Helmholtz free energy

$$\Phi(\tau, \delta) := \frac{A_m}{R_m T} = \frac{A}{RT} = \Phi^o(\tau, \delta) + \Phi^r(\tau, \delta) \tag{1}$$

where $R_m = 8.314\,471\ \mathrm{J \cdot mol \cdot K^{-1}}$ is the universal gas constant according to Moldover et al. [9], A_m the molar free energy, A the specific free energy, $R = R_m/M$ the individual gas constant, $M = 0.066\,051\ \mathrm{kg \cdot mol^{-1}}$ the molar mass, $\tau = T_0/T$ the inverse reduced temperature, and $\delta = \varrho/\varrho_0$ the reduced density. The reducing constants for temperature and density are $T_0 = 386.41$ K and $\varrho_0 = 368\ \mathrm{kg \cdot m^{-3}}$. They correspond to the critical parameters T_c and ϱ_c determined by Higashi et al. [10].

The dimensionless form Φ of the fundamental equation of state is split into an ideal part Φ^o describing ideal-gas properties and into a residual part Φ^r taking into account the behavior of the real fluid. The ideal part Φ^o of the fundamental equation of state is analytically derived from the ideal-gas law and an equation for the isobaric heat capacity c_p^o of the ideal gas. In the first step the c_p^o equation was based on experimental ideal-gas heat capacities. In subsequent steps of optimization, that preliminary c_p^o equation was improved by fitting it simultaneously with the residual part Φ^r to the c_p values of Porichanskii et al. [7]. The final function of the ideal part Φ^o resulted in

$$\Phi^o(\tau, \delta) = a_1^o + a_2^o \tau - \ln \tau + \ln \delta + a_3^o \tau^{-1/4} + a_4^o \tau^{-2} + a_5^o \tau^{-4} \tag{2}$$

where $a_1^o = 10.87227$, $a_2^o = 6.839515$, $a_3^o = -20.78887$, $a_4^o = -0.6539092$, and $a_5^o = 0.03342831$. The coefficients a_1^o and a_2^o were determined by setting enthalpy and entropy to $h^* = 200\ \mathrm{kJ \cdot kg^{-1}}$ and $s^* = 1\ \mathrm{kJ \cdot kg^{-1} \cdot K^{-1}}$ for saturated liquid at $T^* = 273.15$ K. This has been carried out after the residual part Φ^r had been established.

In contrast to the simplicity of formulating the ideal part of the Helmholtz free energy, establishing a function for the residual part is generally an optimization process where a suitable function must be found representing the experimental data with the lowest standard deviation possible. Two optimization strategies have been employed to establish the residual part $\Phi^r(\tau, \delta)$ of the fundamental equation of state for HFC-152a. The first one is the regression analysis developed by Wagner [11], which was used to find a suitable structure of the residual part function. During a subsequent nonlinear optimization the coefficients of this equation were readjusted by fitting them directly to the selected experimental data according to the method proposed by Ahrendts and Baehr [12]. Further information on the optimization process is given by Tillner-Roth [1]. The final function for the residual part Φ^r is written as

$$\Phi^r(\tau, \delta) = \sum_{i=1}^{7} a_i \tau^{t_i} \delta^{d_i} + \exp(-\delta) \sum_{i=8}^{11} a_i \tau^{t_i} \delta^{d_i} + \exp(-\delta^2) \sum_{i=12}^{15} a_i \tau^{t_i} \delta^{d_i} + \exp(-\delta^3) \sum_{i=16}^{19} a_i \tau^{t_i} \delta^{d_i} \tag{3}$$

The coefficients a_i and the exponents t_i and d_i are listed in Table I.

Table I. Coefficients and Exponents of the Residual Part $\Phi^r(\tau, \delta)$ for HFC-152a

i	a_i	t_i	d_i
1	0.3552260	0	1
2	-0.1425660×10^{1}	3/2	1
3	$-0.4631621 \times 10^{-1}$	3	1
4	0.6903546×10^{-1}	−1/2	3/2
5	0.1975710×10^{-1}	−1/2	3
6	0.7486977×10^{-3}	−1/2	6
7	0.4642204×10^{-3}	3/2	6
8	−0.2603396	3	1
9	$-0.7624212 \times 10^{-1}$	4	1
10	0.2233522	3	3
11	0.1992515×10^{-1}	2	4
12	0.3449040	4	1
13	−0.4963849	5	1
14	0.1290719	6	1
15	0.9760790×10^{-3}	5	8
16	0.5066545×10^{-2}	25/2	2
17	$-0.1402020 \times 10^{-1}$	25	3
18	0.5169918×10^{-2}	20	5
19	0.2679087×10^{-3}	25	6

4. REPRESENTATION OF THERMODYNAMIC PROPERTIES

In the subsequent paragraphs the representation of the thermodynamic surface of HFC-152a by the new fundamental equation of state (referred to as EOS) is discussed by comparing it with experimental data and to the equation of state established by Tamatsu et al. [13], which is referred to as TSW-EOS. Not all experimental results used for this work were available to Tamatsu et al., which explains most differences between the two equations of state. Only a selection of comparisons is presented. In Figs. 2 and 5 the results from the TSW-EOS below 230 K are plotted as dashed lines since in this region no experimental data were used by Tamatsu et al. [13].

4.1. (p–ϱ–T) Properties

In Fig. 1, deviations of measured densities in the vapor region at densities $\varrho \leqslant 250$ kg · m^{-3} from the new EOS are shown. The results of Tillner-Roth and Baehr [4] and those of Dressner and Bier [6], to which the EOS has been fitted, agree within ± 0.1% and are represented within the same narrow limits. Beside these data, the results of Majima et al. [14], Tamatsu et al. [15], and Zhao et al. [16] are included. While the data of Tamatsu et al. [15] agree with the new EOS within ± 0.2%, those of Zhao et al. [16] and of Majima et al. [14] show large deviations, occasionally reaching about 1%. Three isobars were calculated from the TSW-EOS, showing excellent agreement at high temperatures but increasing deviations

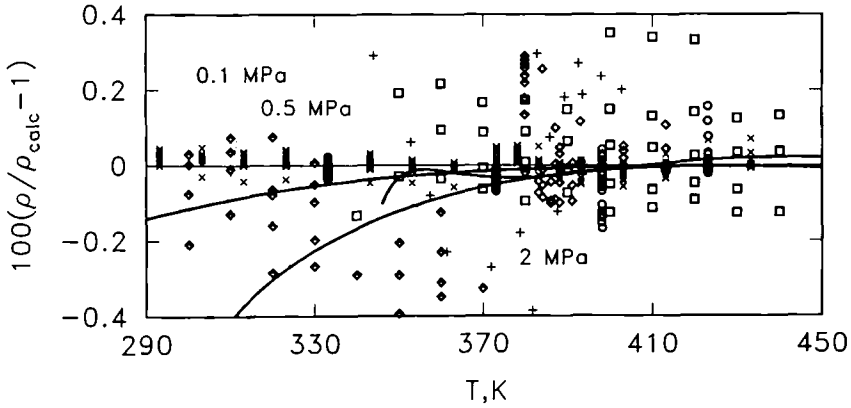

Fig. 1. Deviations between measured densities and values calculated from the present EOS in the gaseous phase for densities $\varrho < 250$ kg m^{-3}. ×, Tillner-Roth and Baehr [4]; ◇, Tillner-Roth and Baehr [3]; ○, Dressner and Bier [6]; □, Tamatsu et al. [15]; +, Zhao et al. [16]; ◆, Majima et al. [14]; — —, TSW-EOS.

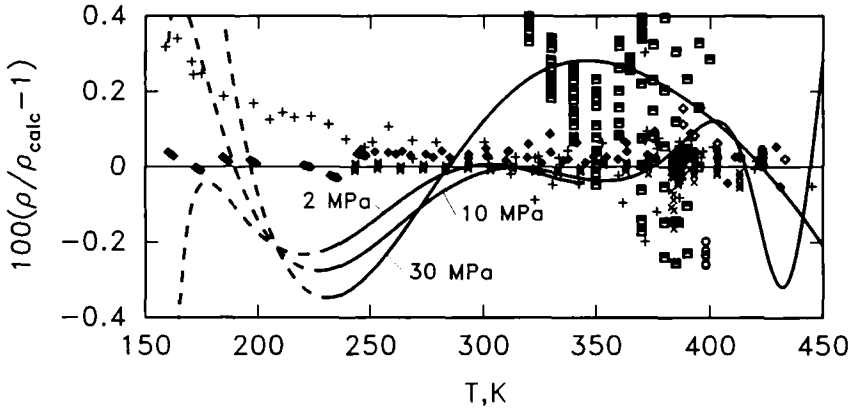

Fig. 2. Deviations between measured densities and values calculated from the present EOS in the liquid for pressures $p < 30$ MPa and densities $\varrho > 500\ \mathrm{kg \cdot m^{-3}}$. ◇, Tillner-Roth and Baehr [4]; ×, Tillner-Roth and Baehr [3]; ○, Dressner and Bier [6]; ◆, Blanke and Weiss [5]; +, Geller et al. [17]; ▭, Iso an Uematsu [18]; ——, TSW-EOS.

for low temperatures. It is assumed that this equation has been fitted to the data of Majima et al. [14] rather than to the more accurate data of Tillner-Roth and Baehr [4].

Deviations for (p–ϱ–T) measurements in the liquid from the EOS are shown in Fig. 2. The densities of Tillner-Roth and Baehr [3] and those of Blanke and Weiss [5], on which the EOS is based, are represented within ±0.1%. Further results were reported by Geller et al. [17], showing positive deviations up to +0.3% at low temperatures and negative deviations at higher temperatures. Large deviations up to 1% are observed for the results obtained by Iso and Uematsu [18]. Systematic deviations up to 0.5% of density are observed between the TSW-EOS and the present EOS in the entire pressure range.

4.2. Isobaric Heat Capacity

In Fig. 3, isobaric heat capacity deviations are shown. The new EOS is based on the results measured by Porichanskii et al. [7] and it reproduces those data within ±2% except some values in the vicinity of the critical temperature on the 5- and 6-MPa isobars. Although the deviations are only about twice the estimated experimental uncertainty, systematic deviations appear among the different isobars, which are particularly large at temperatures above 400 K. Comparison with the TSW-EOS reveals large deviations, up to 6%, which are nearly independent of pressure. Beside the

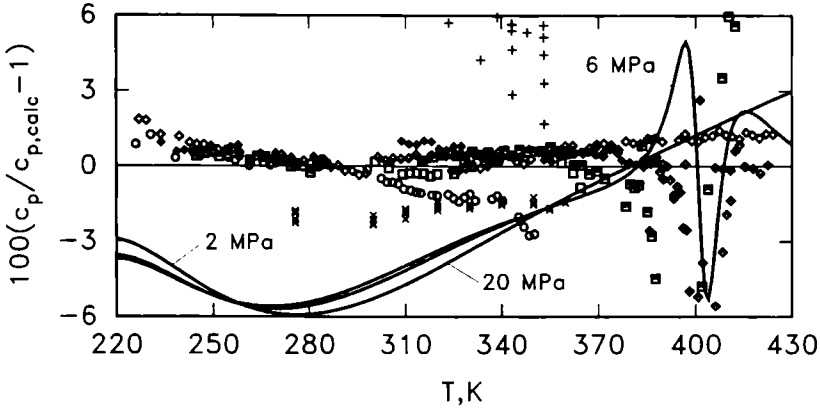

Fig. 3. Deviations between isobaric heat capacities in the liquid and values calculated from the present EOS for pressures $p < 20$ MPa. Porichanskii et al. [7]: ○, 2 MPa; □, 3 MPa; ▭, 5 MPa; ◇, 6 MPa; ◆, 10 MPa; ◈, 15 MPa; ◇, 20 MPa; +, Kubota et al. [20]; ×, Nakagawa et al. [19]; ——, TSW-EOS.

c_p values of Porichanskii et al. [7], results of Nakagawa et al. [19] and of Kubota et al. [20] are included in Fig. 3. Both sets of data differ significantly from the results of Porichanskii et al. [7].

4.3. Vapor Pressure

Deviations between measured and calculated vapor pressures are shown in Fig. 4. The EOS is based on the results of Baehr and Tillner-Roth [8] and of Blanke and Weiss [5], which are represented within ±0.05% or 50 Pa, whichever is greater. Good agreement, within ±0.1%, is also observed with the results of Higashi et al. [10]. Other results show larger deviations but generally confirm the selected values. The vapor pressure predicted by the TSW-EOS shows large systematic deviation from the measured values and from the new correlation.

4.4. Saturated Liquid Density

Saturated liquid densities are shown in Fig. 5. The EOS gives an excellent representation, within ±0.05%, of the results reported by Blanke and Weiss [5] and of those of Tillner-Roth and Baehr [3], which were derived from their liquid densities shown in Fig. 2. Saturated liquid densities from other sources show systematic deviations up to ±0.4%. The densities predicted by the TSW-EOS agree within ±0.2% with the new

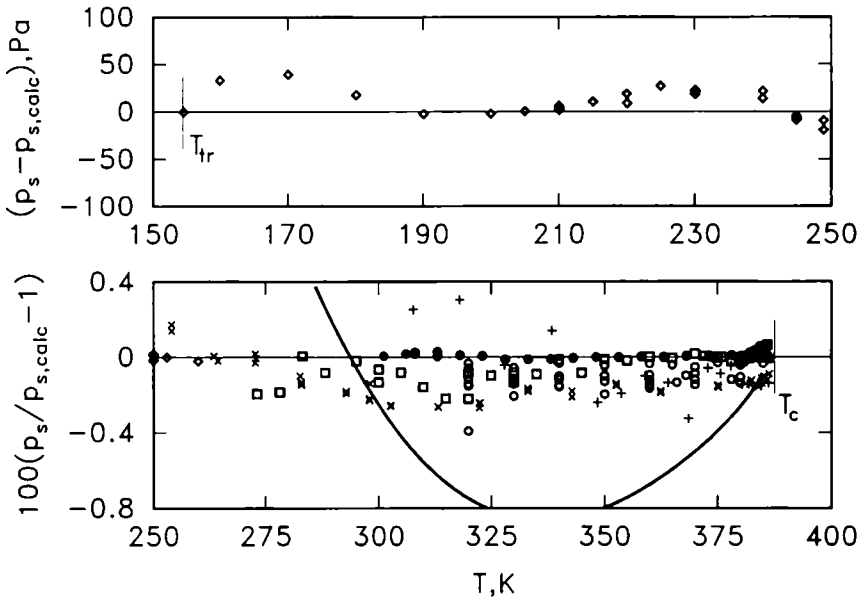

Fig. 4. Deviations between measured vapor pressures and values calculated from the present EOS. ●, Baehr and Tillner-Roth [8]; ◇, Blanke and Weiss [5]; ○, Tamatsu et al. [15]; □, Higashi et al. [10]; +, Takahashi et al. [21]; ×, Bier [22]; ——, TSW-EOS.

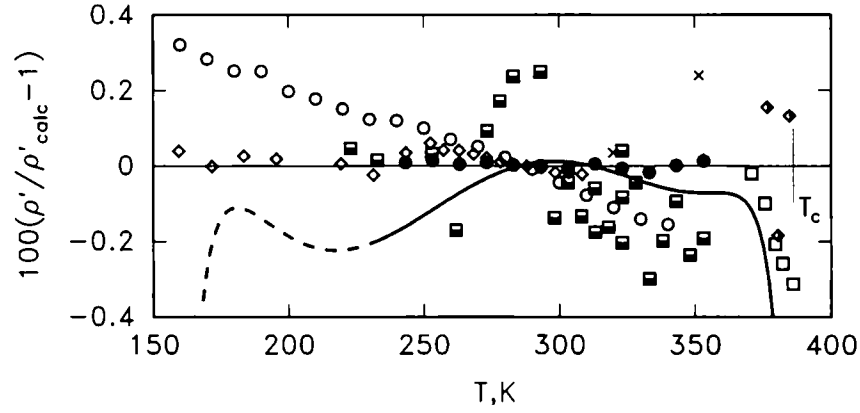

Fig. 5. Deviations between measured saturated liquid densities and values calculated from the present EOS. ●, Baehr and Tillner-Roth [8]; ◇, Blanke and Weiss [5]; ○, Geller et al. [23]; □, Higashi et al. [10]; ■, Sato et al. [24]; ×, Zhao et al. [16]; ◆, Wang et al. [25]; ——, TSW-EOS.

correlation for temperatures above 230 K. Increasing differences are observed when the critical point is approached, which is often observed when comparing equations of state.

5. CONCLUSION

A new equation of state for HFC-152a is presented which is valid for temperatures between 154.56 and 435 K at pressures up to 30 MPa. It is based on a data set comprising (p–ϱ–T) data, isobaric heat capacities, vapor pressures, and saturated liquid densities. Comparisons with experimental data prove the high accuracy of the new equation of state, which therefore allows a reliable calculation of the thermodynamic properties of HFC-152a for most technical applications.

REFERENCES

1. R. Tillner-Roth, *Thermodynamic Properties of R 134a, R 152a and Their Mixtures—Measurements and Fundamental Equations of State*, Forsch.-Ber. DKV Nr. 41 (DKV, Stuttgart, 1993) (in German).
2. T. Hozumi, T. Koga, H. Sato, and K. Watanabe, *Int. J. Thermophys.* **14**:739 (1993).
3. R. Tillner-Roth and H. D. Baehr, *J. Chem. Thermodyn.* **25**:277 (1993).
4. R. Tillner-Roth and H. D. Baehr, *J. Chem. Thermodyn.* **24**:413 (1992).
5. W. Blanke and R. Weiss, *Fluid Phase Equil.* **80**:179 (1992).
6. M. Dressner and K. Bier, *Thermal Mixing Effects in Binary Gaseous Mixtures of New Refrigerants*, Fortschr.-Ber. VDI, Series 3, No. 332 (Düsseldorf, 1993) (in German).
7. E. G. Porichanskii, O. P. Ponomareva, and P. I. Svetlichnyi, *Izv. Vys. Ucheb. Zaved. Energ.* **3**:122 (1982).
8. H. D. Baehr and R. Tillner-Roth, *J. Chem. Thermodyn.* **23**:1063 (1991).
9. M. R. Moldover, J. P. M. Trusler, T. J. Edwards, J. B. Mehl, and R. S. Davis, *J. Res. Natl. Bur. Stand.* **93**:85 (1988).
10. Y. Higashi, M. Ashizawa, Y. Kabata, T. Majima, M. Uematsu, and K. Watanabe, *JSME Int. J.* **30**:1106 (1987).
11. W. Wagner, *A Statistical Method for Establishing Thermodynamic Equations of State—Applied to the Vapour Pressure Curve of Pure Substances*, Fortschr.-Ber. VDI, Series 3, No. 39 (Düsseldorf, 1974) (in German).
12. J. Ahrendts and H. D. Baehr, *Int. J. Chem. Eng.* **21**:557 (1981).
13. T. Tamatsu, H. Sato, and K. Watanabe, *Int. J. Refrig.* **16**:347 (1993).
14. T. Majima, M. Uematsu, and K. Watanabe, *Proc. 8th Jap. Symp. Thermophys. Prop.* **8**:77 (1987).
15. T. Tamatsu, T. Sato, H. Sato, and K. Watanabe, *Int. J. Thermophys.* **13**:985 (1992).
16. Z. Y. Zhao, J. M. Yin, and L. C. Tan, *Fluid Phase Equil.* **80**:191 (1992).
17. V. Z. Geller, E. G. Porichanskii, P. I. Svetlichnyi, and Y. G. Elkin, *Kholod. Tekh.* **29**:43 (1979).
18. A. Iso and M. Uematsu, *Physica A* **156**:454 (1989).
19. S. Nakagawa, T. Hori, H. Sato, and K. Watanabe, *J. Chem. Eng. Data* **38**:70 (1993).
20. H. Kubota, H. Sugitani, Y. Tanaka, and T. Makita, *Chemistry Express* Kinki Chemical Society, Japan, 1987), Vol. 2, p. 397.

21. M. Takahashi, C. Yokoyama, and S. Takahashi, *Proc. 7th Jap. Symp. Thermophys. Prop.* (1986), pp. 179–182.
22. K. Bier, personal communication, University of Karlsruhe (1990).
23. V. Z. Geller, E. G. Porichanskii, P. I. Svetlichnyi, and Y. G. Elkin, *Kholod. Tekh.* **2**:42 (1980).
24. H. Sato, M. Uematsu, and K. Watanabe, *Fluid Phase Equil.* **36**:167 (1987).
25. J. Wang, Z. G. Liu, L. C. Tan, and J. M. Yin, *Fluid Phase Equil.* **80**:203 (1992).